The EMBO Journal (2011) 30, 4371–4386 | © 2011 European Molecular Biology Organization | All Rights Reserved 0261-4189/11
www.embojournal.org

THE EMBO JOURNAL

Optic atrophy 1 is an A-kinase anchoring protein on lipid droplets that mediates adrenergic control of lipolysis

Guillaume Pidoux[1,2,7,8], Oliwia Witczak[1,2,3,7], Elisabeth Jarnæss[1,2,9], Linda Myrvold[1,2,3,10], Henning Urlaub[4,5], Anne Jorunn Stokka[1,2], Thomas Küntziger[6] and Kjetil Taskén[1,2,*]

[1]Centre for Molecular Medicine Norway, Nordic EMBL Partnership, University of Oslo, Oslo, Norway, [2]Biotechnology Centre, University of Oslo, Oslo, Norway, [3]Faculty of Health Sciences, Oslo and Akershus University College of Applied Sciences, Oslo, Norway, [4]Max Planck Institute for Biophysical Chemistry, Bioanalytical Mass Spectrometry Group, Göttingen, Germany [5]Bioanalytics, Department of Clinical Chemistry, University Medical Center Göttingen, Göttingen, Germany and [6]Institute of Basic Medical Sciences, University of Oslo, Oslo, Norway

Adrenergic stimulation of adipocytes yields a cAMP signal that activates protein kinase A (PKA). PKA phosphorylates perilipin, a protein localized on the surface of lipid droplets that serves as a gatekeeper to regulate access of lipases converting stored triglycerides to free fatty acids and glycerol in a phosphorylation-dependent manner. Here, we report a new function for optic atrophy 1 (OPA1), a protein known to regulate mitochondrial dynamics, as a dual-specificity A-kinase anchoring protein associated with lipid droplets. By a variety of protein interaction assays, immunoprecipitation and immunolocalization experiments, we show that OPA1 organizes a supramolecular complex containing both PKA and perilipin. Furthermore, by a combination of siRNA-mediated knockdown, reconstitution experiments using full-length OPA1 with or without the ability to bind PKA or truncated OPA1 fused to a lipid droplet targeting domain and cellular delivery of PKA anchoring disruptor peptides, we demonstrate that OPA1 targeting of PKA to lipid droplets is necessary for hormonal control of perilipin phosphorylation and lipolysis.

The EMBO Journal (2011) **30,** 4371–4386. doi:10.1038/emboj.2011.365; Published online 7 October 2011
Subject Categories: membranes & transport; cellular metabolism
Keywords: cAMP; cell signalling; lipolysis; OPA1; perilipin

*Corresponding author. Centre for Molecular Medicine Norway, Nordic EMBL Partnership and Biotechnology Centre, University of Oslo, PO Box 1125, Blindern, 0317 Oslo, Norway. Tel.: +47 2284 0505; Fax: +47 2284 0506; E-mail: kjetil.tasken@biotek.uio.no
[7]These authors contributed equally to this work
[8]Present address: INSERM U767 and PremUp, Université Paris Descartes, Paris F-75006, France
[9]Present address: Axis-Shield ASA, Oslo, Norway
[10]Present address: Oslo University Hospital, Oslo, Norway

Received: 24 July 2011; accepted: 7 September 2011; published online: 7 October 2011

Introduction

In the fed state, the normal physiological response of white adipose tissue (WAT) to insulin involves generation of triacylglycerol (TAG) from free, nonesterified fatty acids (FFA) and glycerol and storage of TAG in intracellular lipid droplets. Lipid droplets consist of a hydrophobic core of TAG, surrounded by a phospholipid and cholesterol monolayer to which numerous proteins are attached. In the fasting state, stimulation of β-adrenergic receptors (β-ARs) with catecholamines either through sympathetic nervous control (noradrenalin), or through hormonal stress responses (adrenalin) or triggering of glucagon receptors on adipocytes initiate a precisely regulated process of lipolysis, which liberates FFA and glycerol to be used as energy substrates by other tissues. The activation of lipolysis proceeds by generation of cAMP leading to activation of protein kinase A (PKA). Subsequently, PKA phosphorylates perilipin (PAT-family member perilipin 1, *PLIN1*; see Kimmel *et al*, 2009 for review of nomenclature), a protein localized on the surface of the TAG-containing lipid droplets. Perilipin serves as a gatekeeper that controls access of lipases to lipid droplets in a phosphorylation-dependent fashion (Fain and Garcija-Sainz, 1983; Greenberg *et al*, 1991, 1993; Blanchette-Mackie *et al*, 1995). In the absence of any stimulus, unphosphorylated perilipin on the surface of lipid droplets blocks access of lipases, thus protecting TAG from lipolysis. Upon phosphorylation, perilipin alters conformation allowing lipases to access lipid droplets and degrade TAG (Brasaemle *et al*, 2000b; Souza *et al*, 2002; Tansey *et al*, 2003). Hence, at times of stress, exercise or fasting, hormone-induced lipolysis is triggered by making lipid droplets accessible for lipases and liberated FFA serves as a fuel for the peripheral tissues of the body (such as the heart and skeletal muscle) (Londos *et al*, 1999; Brasaemle *et al*, 2000a). Furthermore, PKA phosphorylates hormone-sensitive lipase (HSL), which was the first substrate for PKA shown to be regulated in hormone-induced lipolysis. HSL was until recently thought to be the enzyme responsible for hydrolysis of stored TAG and to control the rate-limiting step in regulation of lipolysis (Fain and Garcija-Sainz, 1983). However, HSL null-mutant mice clearly demonstrated that HSL is dispensable as a substantial fraction of catecholamine-stimulated lipolysis as well as basal lipolysis remain unaffected (Osuga *et al*, 2000; Wang *et al*, 2001; Haemmerle *et al*, 2002). Even more recent studies have identified desnutrin/adipocyte triglyceride lipase (ATGL) as the most important enzyme for degradation of TAG (Zimmermann *et al*, 2003, 2004; Jenkins *et al*, 2004; Villena *et al*, 2004). TAG hydrolase (TGH) may also contribute to non-HSL TAG lipolysis (Soni *et al*, 2004). Desnutrin/ATGL and TGH are, however, not regulated by phosphorylation. Together with the fact that HSL is dispensable in catecholamine-stimulated lipolysis, these results point to the gatekeeper function of perilipin as an important regulatory mechanism. However, HSL appears

to be the only enzyme degrading diacylglycerol to FFA and monoacylglycerol, which is then hydrolysed to FFA and glycerol by monoglyceride lipase, but these reactions proceed comparably faster than the TAG hydrolysis, which remains the rate-limiting step in the control of lipolysis (Giudicelli *et al*, 1974; Tornqvist and Belfrage, 1976; Fredrikson *et al*, 1986).

The localization of PKA holoenzyme within the cell is controlled by interactions between the regulatory (R) subunit dimer of PKA and A-kinase anchoring proteins (AKAPs) (Diviani and Scott, 2001; Michel and Scott, 2002; Tasken and Aandahl, 2004). AKAPs target pools of PKA type I and type II (distinguished by the type I or type II R subunit, RI or RII) to distinct subcellular loci and facilitate discrete spatial and temporal control of phosphorylation of specific substrates. They also scaffold supramolecular signalling complexes with multiple signalling enzymes. All AKAPs contain an A-kinase-binding (AKB) domain and a unique targeting domain directing the PKA–AKAP complex to defined subcellular structures, membranes or organelles (Carr *et al*, 1992; Wong and Scott, 2004; Gold *et al*, 2006; Kinderman *et al*, 2006; Pidoux and Tasken, 2010).

Some studies have suggested the presence of AKAPs associated with lipid droplets to trigger lipolysis by discrete control of perilipin phosphorylation (Zhang *et al*, 2005; Bridges *et al*, 2006). However, no AKAP targeting a pool of PKA to lipid droplets and controlling the induction of lipolysis via phosphorylation of perilipin has been identified to date. In this study, we show that the previously identified mitochondrial protein optic atrophy 1 (OPA1) also functions as a dual-specificity AKAP (binding both type I and type II PKA) associated with lipid droplets. Mutations in the *opa1* gene is the predominant cause of autosomal dominant optic atrophy, a progressive form of bilateral blindness caused by loss of retinal ganglion cells and atrophy of the optic nerve (Alexander *et al*, 2000; Delettre *et al*, 2000). Previous studies have shown OPA1 to be a dynamin-related GTPase required for mitochondrial fusion, and regulation of apoptosis and localized both on the inner membrane of mitochondria and on cristae (Sesaki *et al*, 2003; Cipolat *et al*, 2004; Frezza *et al*, 2006; Ishihara *et al*, 2006). Here, we report the presence of OPA1 in adipocytes, where it is associated with both mitochondria and lipid droplets. We find that OPA1 forms a complex with PKA and perilipin on lipid droplets. Finally, we assign a new function to OPA1 by showing that it is involved in the control of lipolysis in response to adrenergic stimuli by anchoring a pool of PKA that phosphorylates perilipin and thereby triggers lipolysis.

Results

OPA1 is an AKAP associated with lipid droplets

To assess the effect of PKA anchoring in adrenergic regulation of lipolysis, 3T3-L1 cells were differentiated into adipocytes and transfected with constructs directing expression of a HA-tagged soluble fragment of AKAP-Lbc encompassing the PKA-binding site (Ht31 anchoring disruptor) or the corresponding control construct with proline substitutions (Ht31-P) that does not bind PKA (Ct in Figure 1A). Subsequently, transfected cells were stimulated with isoproterenol to activate PKA and perilipin phosphorylation status examined in immunoprecipitates from total cell extracts using an anti-RRXpS/T antibody detecting phosphorylated PKA substrates (Figure 1A). While isoproterenol-induced perilipin phosphorylation was observed in Ht31-P-transfected cells, expression of the Ht31 anchoring disruptor abolished phosphorylation without affecting the level of immunoprecipitated perilipin. This suggests that an AKAP targets PKA to facilitate discrete adrenergic control of perilipin phosphorylation. In search of an AKAP for perilipin, lipid droplets were purified by sucrose gradient fractionation of lysates from differentiated 3T3-L1 adipocytes and lipid droplet protein extracts submitted to overlay with radiolabelled RII in the absence and presence of Ht31 anchoring disruptor peptide (Figure 1B). Five bands with molecular masses of ~110, 90, 75, 50 and 40 kDa detected by RII-overlay and competed by Ht31 peptide appeared to be enriched in lipid droplets compared with cell lysates from 3T3-L1 cells. Proteins in the regions of corresponding mobility from parallel lanes in the gel were excised, subjected to tryptic digestion and analysed by mass spectrometry (Supplementary Table SI).

Curation of lists of identified proteins from several experiments and bioinformatic analysis to identify proteins with putative PKA-binding sites resulted in a list of nine AKAP candidates. Libraries of overlapping peptides covering the putative PKA-binding sites of the candidates were synthesized on solid phase and subjected to RII-overlay in the absence and presence of Ht31 peptide (Figure 1C). The amphipathic helix AKB from AKAP-KL was included as a positive control. This analysis identified a sequence in the C-terminal part of a protein called OPA1 that bound RII in an Ht31-dependent manner. This suggests that OPA1 is a putative AKAP and that, in addition to its mitochondrial localization, OPA1 can also be associated with lipid droplets in adipocytes. To confirm and extend these results, the C-terminal part of the OPA1 sequence mapped in Figure 1C was synthesized as 19 mer overlapping peptides with 1-amino-acid offset on solid phase and analysed for PKA binding by RI- and RII-overlay with or without Ht31. This identified a sequence binding both RI and RII in the C-terminal part of OPA1 (amino acids 940–958; Figure 1D). Modelling the sequence of amino acids 940–958 in OPA1 as an α-helix in a helical wheel configuration suggested that the AKB sequence is an amphipathic helix with one clearly defined hydrophobic face and a negatively charged polar face, which is characteristic of AKB regions in AKAPs (Figure 1E, left). Furthermore, proline substitutions in the sequence (V942P, I945P, L949P; peptide OPA1 940–958-3P) that distort the α-helical configuration abolished binding to PKA (Figure 1E, right).

We have previously developed an amplified luminescence ligand proximity assay (AlphaScreen) based on RI binding to D-AKAP1 that can be used to characterize AKB regions in AKAPs as competitors (Stokka *et al*, 2006; Jarnaess *et al*, 2008). Since OPA1 appeared to bind both RI and RII, we used this RI competition binding platform to evaluate the binding properties of OPA1. As shown in Figure 1F, a peptide corresponding to amino acids 940–958 in OPA1 as well as Ht31 competed RI binding to D-AKAP1 with IC_{50}-values of 8.1 ± 0.13 and $9.5 \pm 0.16\,\mu M$, respectively, in line with earlier observations with RI using this assay (Jarnaess *et al*, 2008). In contrast, the OPA1 940–958-3P control peptide was not able to compete the D-AKAP-RI interaction confirming the observation in Figure 1E. Taken together, our results suggest

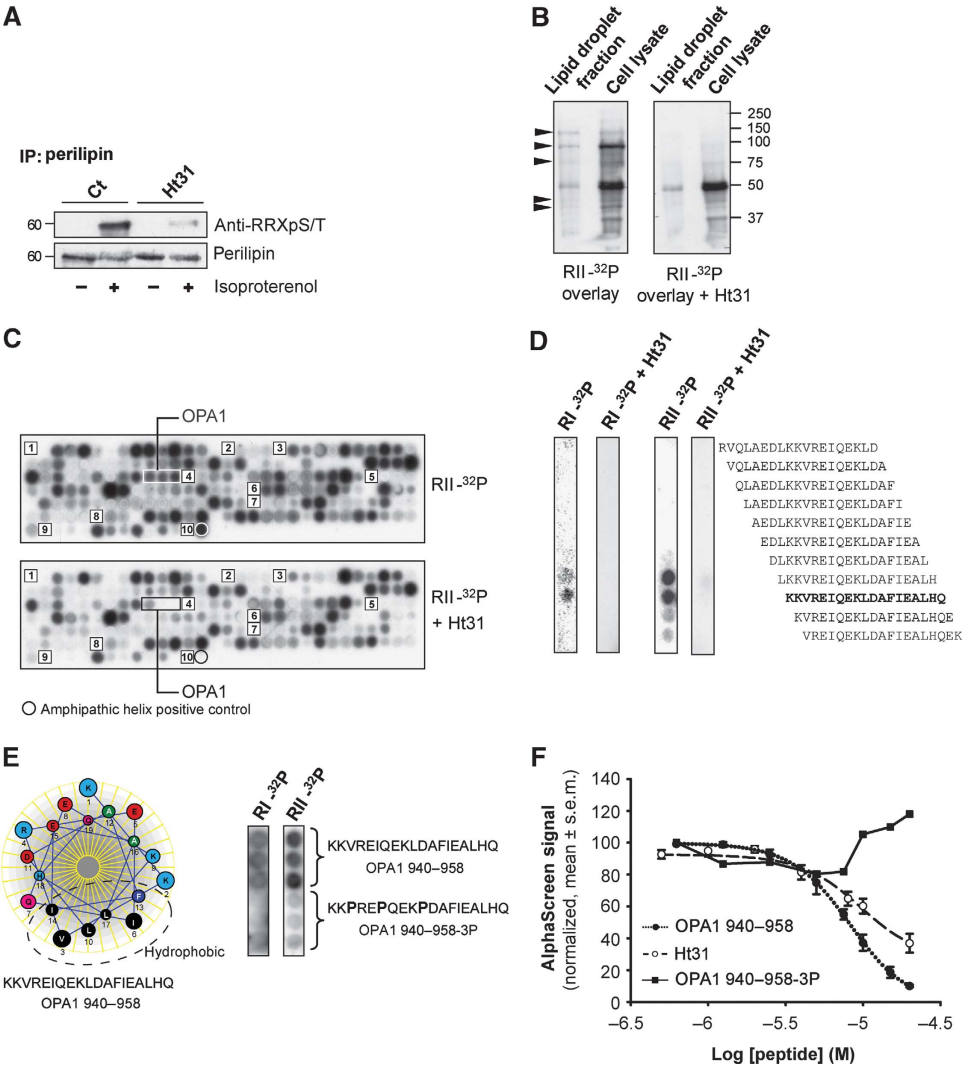

Figure 1 OPA1 is an AKAP associated with lipid droplets. (**A**) Perilipin was immunoprecipitated from extracts of 3T3-L1 fibroblasts differentiated into adipocytes, transfected with a mammalian expression vector encoding Ht31 or Ht31-P (Ct), and stimulated with or without isoproterenol (+, −). Perilipin phosphorylation status was assessed by immunoblotting for phosphorylated PKA substrates (anti-RRXpS/T antibody) and perilipin. (**B**) Purified lipid droplets and total cell lysates from 3T3-L1 adipocytes were subjected to a solid phase binding assay using ^{32}P-radiolabelled RII (RII-overlay) as a probe in the absence (left panel) or presence (right panel) of the Ht31 anchoring disruptor peptide (500 nM). Arrows indicate regions with putative AKAPs, which were excised from parallel lanes, and analysed by mass spectrometry. (**C**) Relevant parts of the sequences of putative AKAPs identified by mass spectrometry were printed on solid phase as overlapping 20 mer peptides (3 amino acid offset) and subjected to RII-overlay in the absence (upper panel) or presence (lower panel) of Ht31 (500 nM). Putative AKAP sequences as identified by numbers on the array are (Swissprot database entry in parenthesis): 1, Dip2b (Q3UH60); 2, Matrin3 (Q9R0U5); 3, OPA1 (P58281); 4, LONP (Q8CGK3); 5, LETM1 (Q9Z210); 6, Hsp90b1 (P08113); 7, importin subunit β1 (P70168); 8, unknown protein product; 9, nuclear myosin 1 β (Q9ERB6); 10, AKAP-KL amphipathic helix (positive control). (**D**) RI- or RII-overlay in the absence or presence of Ht31 anchoring disruptor peptide (500 nM) of array of immobilized OPA1 19 mer peptides (1 amino acid offset). Bold sequence: PKA-R-binding region in OPA1. (**E**) α-Helical wheel representation of the PKA-R binding sequence contained within amino acids 940–958 of OPA1 (left). Dashed line indicates a hydrophobic region. R-overlays of the immobilized OPA1 940–958 substituted sequence with three prolines introduced (OPA1 940–958-3P) (right). (**F**) Concentration-dependent competition of RIα interaction with GST-D-AKAP1 (20 nM each) by OPA1 940–958 (●), HT31 (○) and OPA1 940–958-3P (■) peptides in a ligand proximity assay (AlphaScreen). Data represent mean ± s.e.m. of three independent experiments performed in duplicate. Figure source data can be found in Supplementary data.

that OPA1 is an AKAP with a PKA-binding domain encompassing amino acids 940–958 in the C-terminal part of the protein that can bind both RI and RII.

Kinetics of the OPA1–PKA interaction

We next determined the rate and affinity constants of the OPA1–PKA association. Real-time analyses were carried out by surface plasmon resonance (SPR) technology (Figure 2). Specifically, cAMP-free RI and RII were immobilized on the surface of a CM5 sensor chip coated with 8-AHA-cAMP and a purified, MBP-fused full-length OPA1 protein (containing the AKB region) was injected over the surfaces. The sensorgrams of MBP-OPA1 binding to RI and RII loaded surfaces (Figure 2A and C, respectively) as well as the corresponding steady-state binding isotherms (Figure 2B and D) clearly demonstrated a concentration-dependent binding with nanomolar affinities for both RI ($K_D = 12.5 \pm 2.8$ nM) and RII ($K_D = 14.0 \pm 1.4$ nM) and with K_D-values consistently somewhat lower for RI than for RII in all experiments. Furthermore, in contrast to observations made with other

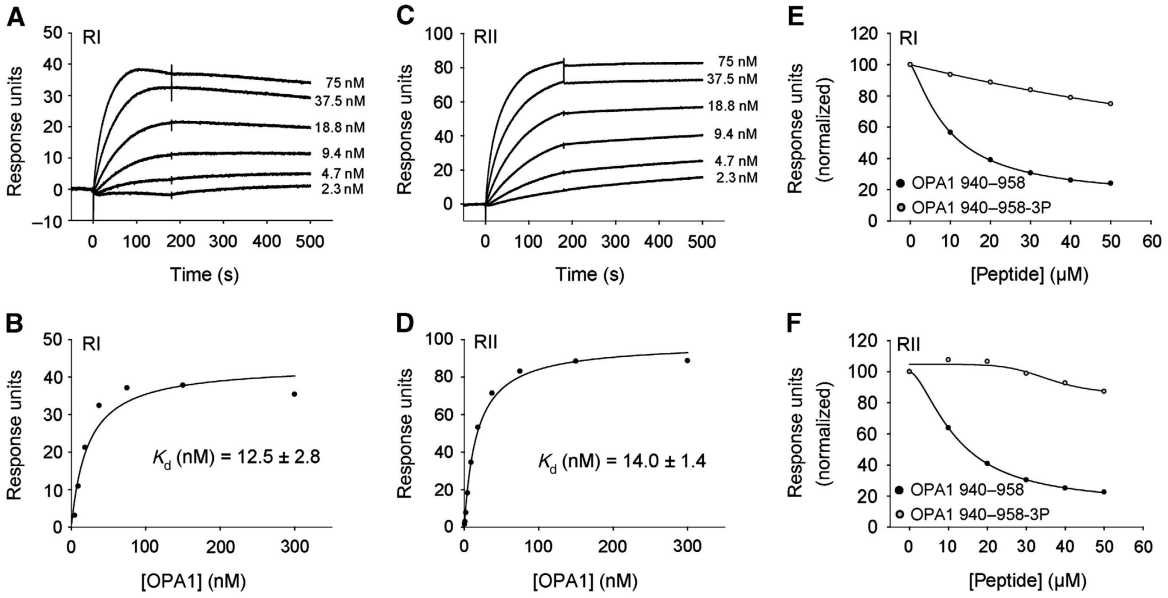

Figure 2 Studies of the OPA1–RI and OPA1–RII interaction. (**A**, **C**) SPR studies of the MBP-OPA1 binding to immobilized PKA-RI (**A**) or PKA-RII (**C**) on a sensor chip coated with 8-aminohexylamino-cAMP. MBP-OPA1 at concentrations indicated was injected for 180 s and the dissociation phase was monitored for 300 s. The graphs are representative of three independent experiments performed on different sensor surfaces. (**B**, **D**) Steady-state binding of the increasing MBP-OPA1 concentrations obtained from (**A**, **C**). The affinity constant was derived assuming a 1:1 binding in a Langmuir model using a global fit analyses algorithm provided in the BIAcore T100 evaluation software. (**E**, **F**) Qualitative surface competition experiments with the OPA1 940–958 peptide. In all, 75 nM MBP-OPA1 was injected on a surface with captured PKA-RI (**E**) or PKA-RII (**F**) in the presence or absence of increasing concentrations (10–50 μM) of the OPA1 940–958 or the OPA1 940–958-3P peptide. Both peptides were also injected without AKAP present and the binding response obtained in the absence of an AKAP present were subtracted in the graph shown. The graphs show one representative experiment of three independent experiments performed on different sensor surfaces.

RI-binding AKAPs, which typically display a faster off-rate for RI, the on- and off-rates of RI and RII binding to OPA1 were similar (RI: $K_a = 6.6 \times 10^5$/M/s, $K_d = 3.7 \times 10^{-4}$/s; RII: $K_a = 1.1 \times 10^6$/M/s, $K_d = 4.4 \times 10^{-4}$/s). Binding of MBP-OPA1 to RI and RII was displaced in the presence of increasing concentrations (10–50 μM) of the OPA1 940–958 peptide characterized in Figure 1F (Figure 2E and F), whereas no displacement was observed with the proline-substituted OPA1 940–958-3P peptide. These results suggest that OPA1 may be a true dual-specificity AKAP.

OPA1 and PKA colocalize on lipid droplets in 3T3-L1 adipocytes

OPA1 expression in brown adipose tissue (BAT) and WAT, liver, muscle and 3T3-L1 adipocytes was analysed by immunoblotting (Figure 3A). This showed high levels of expression of three different forms in BAT and 3T3-L1 adipocytes whereas only the high and low molecular weight isoforms were detected at lower levels of expression in WAT. Liver and muscle also expressed OPA1 isoforms of different mobility. In contrast, perilipin was only expressed in adipose tissue and 3T3-L1 adipocytes. The level of expression of OPA1 could relate to the number of mitochondria, for example, in BAT versus WAT as OPA1 is previously reported to be localized in mitochondria.

The expression of OPA1 was next analysed during differentiation of 3T3-L1 preadipocytes into adipocytes (Figure 3B). Whereas the expression of the different R isoforms RIα, RIIβ remained constant during the differentiation process, the expression of OPA1 was upregulated somewhat prior to or concomitantly with the appearance of perilipin, which could indicate regulation of OPA1 during adipocyte development by transcription factors such as PPARγ to match that of other lipid droplet proteins. In contrast, mitochondrial proteins such as mitofilin and mitofusin 2 were not regulated with the same kinetics or amplitude, suggesting that the observed regulation of OPA1 is not just a function of an increase in the number of mitochondria.

The subcellular localization of OPA1 versus perilipin and PKA in adipocytes was analysed by dual-immunofluorescent labelling followed by laser confocal analysis and the extent of overlap was measured using line plot profile and intensity correlation coefficient-based analysis (Bolte and Cordelieres, 2006). OPA1 showed extensive colocalization with perilipin on lipid droplets (Figure 3C–E′; $R = 0.91$). Moreover, studies of the localization of PKA type I (RIα) and type II (RIIβ) in 3T3-L1 adipocytes demonstrated RIα to have strong colocalization with perilipin on the surface of lipid droplets (Figure 3F–H′; $R = 0.85$). In contrast, RIIβ appeared more localized in the cytoplasm and showed only partial overlap with perilipin on lipid droplets (Figure 3I–K′; $R = 0.67$). In agreement with previous studies, the localization of HSL was found to be mainly in the cytoplasm, but showed also some extent of colocalization with perilipin on lipid droplets (Figure 3L–N′; $R = 0.76$) (Londos *et al*, 1999; Brasaemle *et al*, 2000a).

To explore the possibility of a direct physical interaction between OPA1 and RIα on lipid droplets, we next solubilized the lipid droplet protein content of differentiated 3T3-L1 cells in a buffer containing detergent and *N*-octyl-β-D-glucoside. Immunoprecipitation of OPA1 revealed the presence of both perilipin and OPA1 in the precipitate (Figure 4A). The reverse immunoprecipitation experiment using a perilipin antibody likewise showed coprecipitation of OPA1 (Figure 4B). Interestingly, immunoprecipitation of RIα coprecipitated

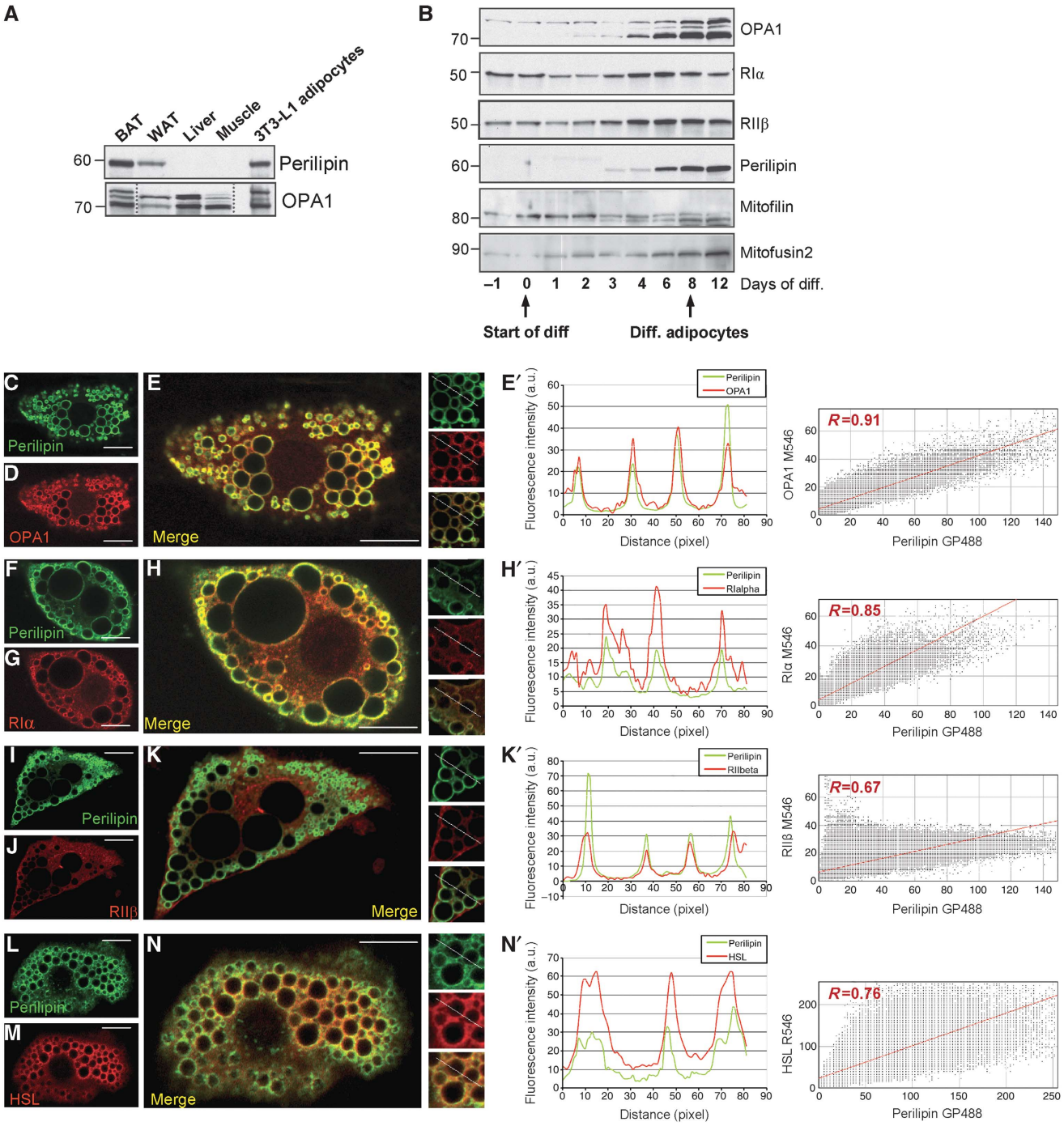

Figure 3 OPA1 is expressed in adipocytes and colocalizes with RIα on lipid droplets. (**A**) Distribution of OPA1 and perilipin in indicated mouse tissues and 3T3-L1 adipocytes by immunoblotting. Dotted lines indicate that an area between the displayed lanes was removed. Shown lanes are from a single gel and exposure. (**B**) Expression of OPA1, RIα, RIIβ, perilipin, mitofilin and mitofusin 2 during the differentiation of 3T3-L1 into adipocytes by immunoblotting. (**C**–**N**′) 3T3-L1 adipocytes were immunostained for perilipin (green; **C**, **F**, **I**, **L**) in combination with OPA1 (red; **D**), RIα (red; **G**), RIIβ (red; **J**) and HSL (red; **M**). Merged pictures are shown in (**E**, **H**, **K**, **N**), respectively. Line plot profile and correlation analysis of colocalization of perilipin with OPA1 (**E**′), RIα (**H**′), RIIβ (**K**′) and HSL (**N**′) are also shown. Plot profiles (middle) show for both channels the variation in fluorescence intensity along line indicated in white in detailed area. Scatter plots (right) show pixel distribution whereby the intensities of a given pixel in the green and red images correspond to the *x*- and *y*-coordinate, respectively. Correlation coefficients (*R*) of overlaps are indicated. Scale bar: 20 μm. Figure source data can be found in Supplementary data.

OPA1 (Figure 4C) and conversely, RIα was detected in OPA1 immunoprecipitates (Figure 4D). In contrast, RIIβ could not be coprecipitated with OPA1 from 3T3-L1 cells (not shown), indicating either that it does not bind in the presence of RI or that the fraction associated with OPA1 is below the level of detection. Moreover, HSL and phospho-HSL were not detected after immunoprecipitation of OPA1 in adipocytes (Figure 4E). Together, our results indicate that OPA1 forms a complex with perilipin and RIα on lipid droplets in 3T3-L1 adipocytes.

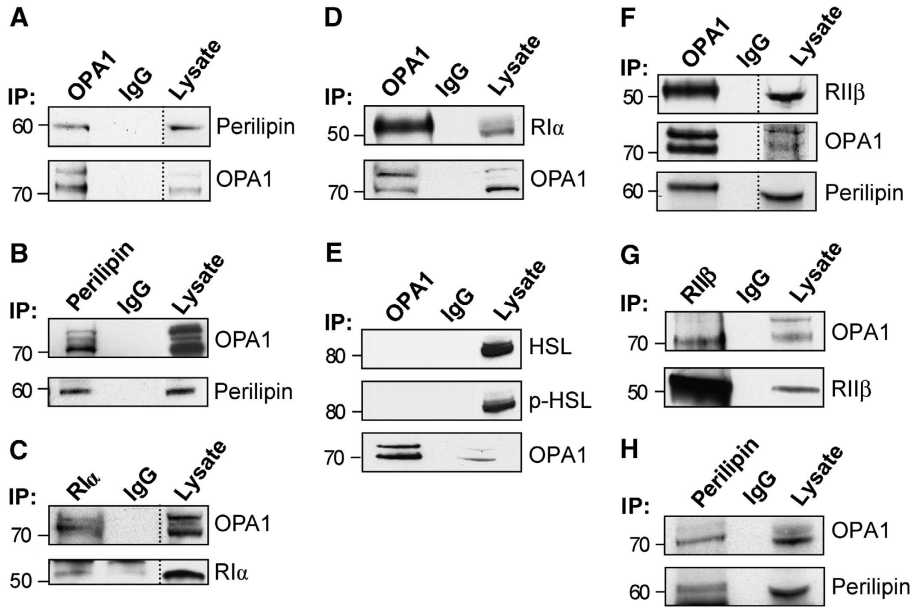

Figure 4 OPA1 organizes a supramolecular complex containing PKA and perilipin. (**A**–**C**) Lysates from 3T3-L1 adipocytes were subjected to immunoprecipitation with OPA1 antibody (**A**, **D**, **E**), perilipin (**B**) and RIα (**C**). Immunoprecipitates and corresponding lysates were analysed by immunoblotting for the presence of the indicated proteins. (**F**, **G**, **H**) Lysates from mouse WAT were subjected to immunoprecipitation with OPA1 (**F**), RIIβ (**G**) or perilipin (**H**) antibodies and analysed for the presence of OPA1, RIIβ and perilipin by immunoblotting. Dotted lines indicate lanes combined from a single gel and exposure. Figure source data can be found in Supplementary data.

While 3T3-L1 adipocytes appear to have an abundance of PKA type I and RI is associated with OPA1, WAT from wild-type mice has been reported to contain mainly PKA type II that regulates lipolysis and with RIIβ being the predominant RII subunit (Cummings *et al*, 1996; Cederberg *et al*, 2001). Therefore, we also examined the pool of PKA associated with OPA1 in total protein extracts from WAT. Here, we found that RII (Figure 4F and G) and not RI (not shown) coimmunoprecipitated with OPA1 and *vice versa*, which is compatible with the notion of OPA1 as a dual-specificity AKAP where the association with type I or type II PKA is determined by the availability of the two isozymes. Furthermore, OPA1 forms a complex with perilipin also in WAT (Figure 4F and H).

OPA1 distribution between lipid droplets and mitochondria

As reports on OPA1 localization and function in cells without lipid droplets describe a mitochondria-associated protein involved in mitochondrial fusion (Cipolat *et al*, 2004; Ishihara *et al*, 2006), it was important to examine the distribution of OPA1 between lipid droplets and mitochondria in adipocytes. Immunostaining of 3T3-L1 adipocytes with perilipin as a marker of lipid droplets was performed together with transfection of the targeting domain of the MDDX28 helicase tagged with the fluorescent protein mCherry (construct ΔMDDX28mCherry) as a marker of the inner mitochondrial membrane, or with immunostaining for mitofusin 2 as a marker of the outer mitochondrial membrane. Laser confocal analysis and intensity correlation coefficient-based analysis revealed little overlap between the lipid droplet marker and mitochondrial markers (Figure 5A–F; Supplementary Figure S1A and B; $R = 0.22$ and 0.43, respectively). In contrast, transfection of 3T3-L1 adipocytes with a construct directing the expression of the full-length OPA1 tagged with green fluorescent protein (GFP-FL-OPA1$^{\#}$) showed specific import of the tagged OPA1 to lipid droplets as evident from a strong overlap with perilipin immunostaining as a marker for lipid droplets (Figure 5G–I; Supplementary Figure S1C; $R = 0.89$), whereas comparably lower intensity signals were detected over mitochondria. This, together with the extensive colocalization of endogenous OPA1 with perilipin (Figure 3C–E′; $R = 0.91$) strongly suggest that OPA1 distribution in adipocytes is not strictly limited to mitochondria and that the main fraction is targeted to lipid droplets together with perilipin.

To determine in more detail the distribution of OPA1 between mitochondria and lipid droplets in adipocytes, post-nuclear supernatants were fractionated by sucrose gradient centrifugation to separate light components with high lipid content such as liposomes from cytoplam and organelles with comparably higher density. Immunoblotting of the resulting fractions (Figure 5J) and quantification by densitometry of the relative distribution from several experiments (Figure 5K) showed perilipin exclusively in fraction 1 corresponding to the lipid droplet position in the density gradient. In contrast, mitochondrial markers for the inner membrane (mitofilin), outer membrane (mitofusin 2) and mitochondrial matrix (pyruvate dehydrogenase E1β subunit) were mainly localized in the bottom fractions, although 10% of mitofilin, 5% of mitofusin 2 and 4% of pyruvate dehydrogenase E1β subunit were also found in the top fraction. These mitochondrial contaminations observed in the lipid droplets fraction could represent mitochondrial membranes from ruptured mitochondria or possibly intact mitochondria weakly associated with lipid droplets. Interestingly, although OPA1 is reported to be a mitochondrial protein in other cell types, its distribution in 3T3-L1 adipocytes with $>80\%$ in the top fractions and $<20\%$ in the bottom fractions is distinctly different from the distribution of the mitochondrial markers in the same experiments. Altogether our results strongly suggest that a significant portion of OPA1 is associated with

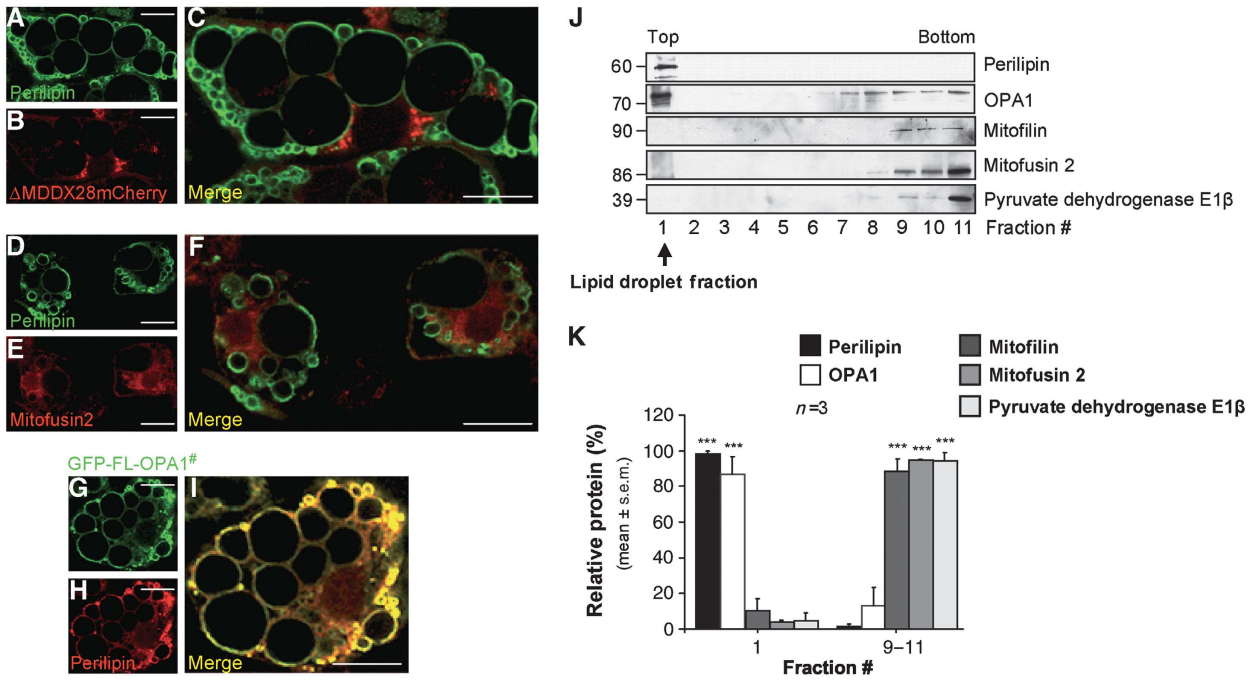

Figure 5 OPA1 distribution between lipid droplets and mitochondria. (**A**–**I**) 3T3-L1 adipocytes were untransfected (**D**–**F**) or transfected with mitochondrial marker ΔMDDX28mCherry (red; **B**) or GFP-OPA1 (green; **G**) and subsequently immunostained for perilipin (green; **A**, **D** and red; **H**) alone or in combination with mitofusin2 antibody (red; **E**). Corresponding merged pictures are shown in (**C**, **F**, **I**). Scale bar: 20 μm. (**J**) Lipid droplets were purified from 3T3-L1 adipocytes by sucrose gradient centrifugation. Fractions were examined by immunoblotting for distribution of perilipin, OPA1, mitofilin (mitochondrial inner membrane marker), mitofusin 2 (mitochondrial outer membrane marker) or pyruvate dehydrogenase E1β subunit (mitochondrial matrix marker). Arrow indicates the mobility of the lipid droplet fraction in the sucrose gradient. One representative experiment of three is shown. (**K**) Relative distribution of the perilipin, OPA1, mitofilin, mitofusin2 and pyruvate dehydrogenase E1β subunit in fraction 1 (lipid droplet fraction) versus fractions 9–11 (mitochondria). Results are expressed as the mean ± s.e.m. of $n=3$ independent experiments (***$P<0.001$). Figure source data can be found in Supplementary data.

the lipid droplet fraction in a mitochondria-independent manner. Furthermore, we also observed a strong colocalization between lipid droplets (perilipin immunolabelling) and GFP-FL-OPA1 (Figure 5G and H; Supplementary Figures S1C and S2A–C′) and GFP-FL-OPA1 with three proline substitutions (V942P, I945P, L949P) inside the AKB domain (GFP-OPA1$^{\#}$ AKBmut) (Supplementary Figure S2D–F′). In addition, deletion of the OPA1 mitochondrial targeting sequence (amino acids 1–87; ΔMTS) as defined in several reports (Misaka *et al*, 2002; Olichon *et al*, 2002; Satoh *et al*, 2003; Kita *et al*, 2009) or deletion of the 30 first critical amino acids of the MTS (Δ1–30) abolish targeting of OPA1 to lipid droplets as well as mitochondria (Supplementary Figure S2G-P′). Furthermore, deletion of the 57 last amino acids of the MTS (Δ30–87) also reduced targeting of OPA1 to both lipid droplets and mitochondria, although to a greater extent for the mitochondrial localization (Supplementary Figure S2Q–V′; $R=0.48$ versus $R=0.26$). These observations suggest that the MTS in OPA1 is important for the targeting of OPA1 also to lipid droplets and that an independent lipid droplet targeting sequence cannot readily be defined.

OPA1 is implicated in the adrenergic control of lipolysis

To address the function of OPA1 as a putative AKAP for perilipin, we employed a combined strategy of RNA interference and rescue with wild-type or modified forms of OPA1 and examined the effect on adrenergic regulation of lipolysis. First, 3T3-L1 adipocytes were transfected with specific OPA1 siRNA or scrambled control, incubated for 24 h, retransfected with OPA1 siRNA and incubated for another 48 h. As shown by immunoblot analysis (Figure 6A), siRNA-mediated knockdown of OPA1 markedly reduced OPA1 protein level by ∼85% after 48–72 h of culture compared with cells transfected with scrambled siRNA ($P<0.025$, $n=3$, see also Supplementary Figure S3A). No difference was seen between control-transfected and untransfected cells, indicating that the method of transfection did not interfere with OPA1 expression nor was it toxic to the differentiated adipocytes. The expression of RIα, RIIβ and HSL remained constant in cells that received OPA1 siRNA, indicating that removal of OPA1 does not affect other components of the PKA signalling pathway. Interestingly, perilipin expression was significantly reduced after siRNA-mediated knockdown of OPA1 by up to 75% at 48 h and 55% at 72 h post-transfection (Supplementary Figure S3B; $P<0.05$). The effect of OPA1 knockdown on perilipin expression may indicate that OPA1 and perilipin interact to stabilize each other and that loss of perilipin expression could result from destabilization of a supramolecular complex. Interestingly, expression of the PAT-family protein ADRP (perilipin 2), but not TIP47 (perilipin 3), appeared to increase two- to three-fold at 48 h, maybe as a rescue mechanism for perilipin downregulation to help preserve lipid droplets (Supplementary Figure S4).

Knockdown of OPA1 protein expression was associated with a significant decrease in isoproterenol-induced glycerol release from 3T3-L1 adipocytes with little adrenergic induction of lipolysis and a 60% reduction in glycerol release compared with scrambled control at 5 or 10 nM isoproterenol

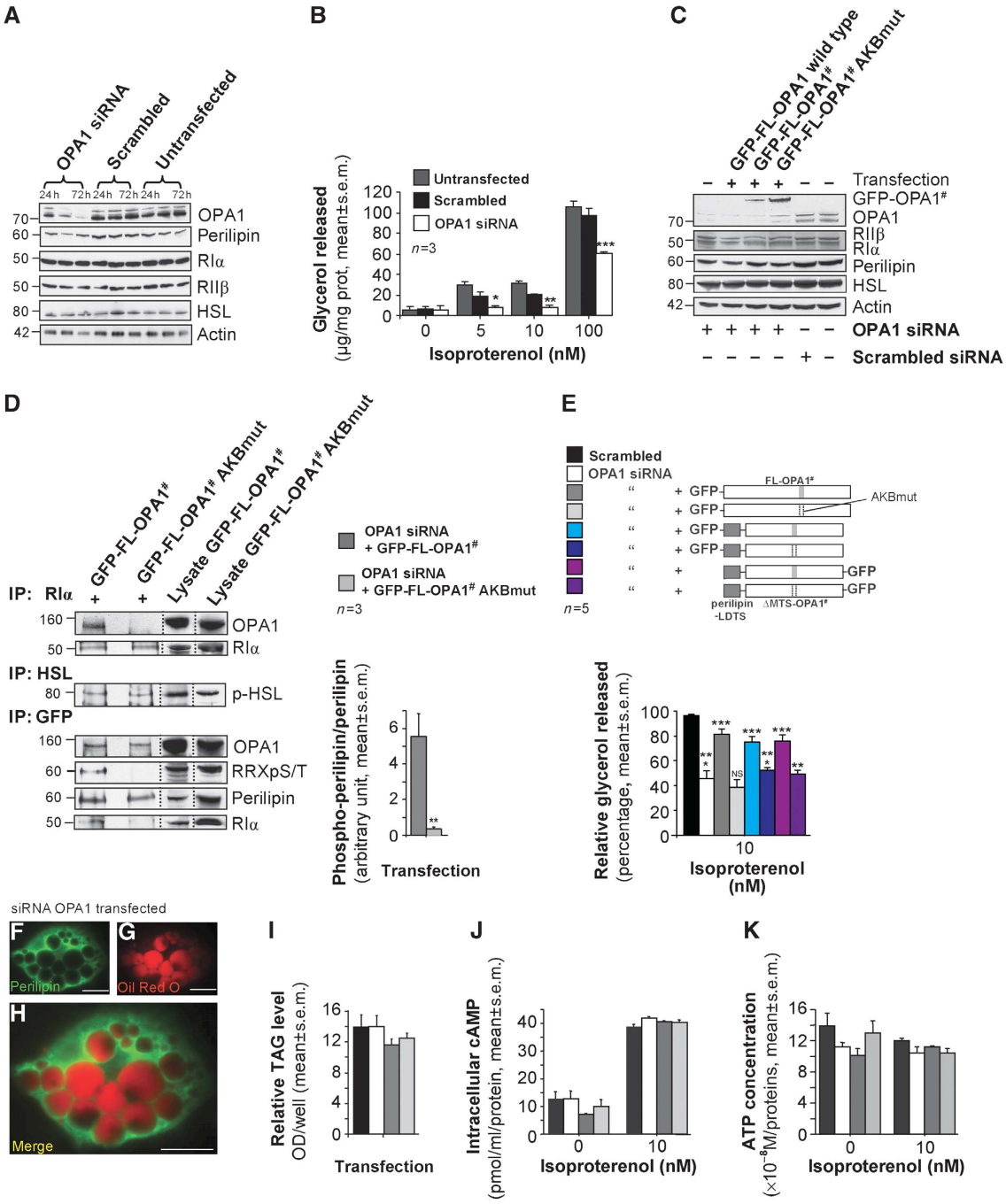

Figure 6 OPA1 is involved in the adrenergic control of lipolysis. (**A**) Immunoblot analysis of OPA1, perilipin, RIα, RIIβ, HSL and actin levels in 3T3-L1 adipocytes transfected with OPA1 siRNA or scrambled control after 24, 48 or 72 h of culture. (**B**) Glycerol release from 3T3-L1 adipocytes after siRNA transfection and stimulation with isoproterenol (5, 10 and 100 nM) for 2 h. (**C**) Detection by immunoblot of OPA1, GFP-FL-OPA1, perilipin, RIα, RIIβ, HSL and actin in 3T3-L1 adipocytes transfected with OPA1-specific siRNA or scrambled control and retransfected with wild-type OPA1-FL-GFP, siRNA-insensitive OPA1-FL-GFP (GFP-FL-OPA1$^{\#}$) or siRNA-insensitive OPA1-GFP 940–958-3P (GFP-FL-OPA1$^{\#}$ AKBmut) plasmids, after 72 h of culture. (**D**; left panel) Lysates from 3T3-L1 adipocytes incubated with OPA1 siRNA and GFP-FL-OPA1$^{\#}$ plasmid or GFP-FL-OPA1$^{\#}$ AKBmut were subjected to immunoprecipitation with RIα, HSL or GFP antibodies. Lysate and precipitate were analysed for the presence of OPA1, RIα, perilipin, phospho-perilipin (PKA substrate antibody (anti-RRXpS/T)) and phospho-HSL. Dotted lines indicate lanes combined from a single gel and exposure. (**D**; right panel) The histogram shows levels of phosphorylated perilipin quantified by densiometry relative to total perilipin levels. (**E**) Amount of glycerol released in the media (percent of maximal) of 3T3-L1 adipocytes during 2 h of stimulation by 10 nM isoproterenol after transfection and incubation with OPA1 siRNA and GFP-FL-OPA1$^{\#}$, GFP-FL-OPA1$^{\#}$ AKBmut or LDTS-ΔMTS-OPA1 chimeric expression vectors for 72 h. (Top) Schematic depiction of constructs. Open box: OPA1 full-length (FL-OPA1$^{\#}$) or deleted of the MTS (ΔMTS-OPA1$^{\#}$); light grey/dotted box: functional or mutated AKB domain (940–958-3P; AKBmut); dark grey box: perilipin lipid droplet targeting sequence (perilipin-LTDS). (**F**–**H**) 3T3-L1 adipocytes were immunostained for perilipin after OPA1 siRNA transfection (green; **F**) in combination with Oil Red O (marker of TAG; red; **G**). (**H**) Merged picture. Scale bar: 20 µm. (**I**) Intracellular TAG content, (**J**) intracellular cAMP content and (**K**) intracellular ATP concentration of 3T3-L1 adipocytes 3 days after incubation with OPA1 siRNA and GFP-FL-OPA1$^{\#}$ plasmid or GFP-FL-OPA1$^{\#}$ AKBmut plasmid. Results represent mean ± s.e.m. of $n=3$ independent experiments except for (**E**) where $n=5$ (***$P<0.001$; **$P<0.01$; *$P<0.05$ and NS, not significant). Figure source data can be found in Supplementary data.

(Figure 6B). The inhibition of isoproterenol-induced lipolysis by OPA1 knockdown was partially overcome at 100 nM where only 37% inhibition compared with control was observed probably because the high cAMP activates PKA over longer distances inside the cell reducing the requirement for AKAP targeting. For this reason, further studies of the effect of manipulation of OPA1 levels on lipolysis were conducted at concentrations around EC_{50} (10–30 nM). To rescue cells with OPA1 knockdown, 3T3-L1 adipocytes were first transfected with OPA1 siRNA to remove endogenous OPA1. This was followed by transfection with mammalian expression vectors encoding wild-type full-length OPA1 fused to green fluorescent protein (GFP-FL-OPA1), GFP-OPA1 made insensitive to functional siRNA (GFP-FL-OPA1$^{\#}$) or GFP-FL-OPA1$^{\#}$ with three proline substitutions (V942P, I945P, L949P) inside the AKB domain (GFP-FL-OPA1$^{\#}$ AKBmut), which should abolish binding of both type I and type II PKA as shown in Figures 1E and F and 2E and F. Whereas cells transfected with an expression vector directing the transcription of an siRNA-sensitive OPA1 did not regain OPA1 expression, adipocytes transfected with vectors directing the expression of siRNA-insensitive GFP-FL-OPA1$^{\#}$ or GFP-FL-OPA1$^{\#}$ AKBmut presented expression of a GFP-FL-OPA1 fusion protein (Figure 6C). Furthermore, colocalization with lipid droplets was confirmed for both these constructs by perilipin immunofluorescent labelling (Figure 5G–I; Supplementary Figures S1C and S2D–F′). While the expression of RIα, RIIβ and HSL remained constant, the expression of perilipin was also found to be decreased in cells transfected with OPA1 siRNA (75% reduction) as previously observed in Figure 6A and in Supplementary Figure S3B, and there was a tendency to reversal of this effect in cells where OPA1 expression was rescued (Supplementary Figure S3C; $P=0.07$).

To assess the ability of the exogenously introduced GFP-FL-OPA1 to form a complex with endogenous PKA and perilipin, immunoprecipitations were performed from cell lysates of adipocytes cotransfected with OPA1 siRNA and siRNA-resistant GFP-FL-OPA1$^{\#}$ or GFP-FL-OPA1$^{\#}$ AKBmut (Figure 6D, left). Immunoprecipitation with RIα revealed the presence of GFP-FL-OPA1 in the precipitate from cells transfected with a vector encoding GFP-FL-OPA1$^{\#}$ but not from cells expressing GFP-FL-OPA1$^{\#}$ AKBmut, whereas RIα was precipitated in both cases. Together with the GFP immunoprecipitation experiment, where RI only coprecipitated with GFP-FL-OPA1$^{\#}$ and not GFP-FL-OPA1$^{\#}$ AKBmut, this indicates that OPA1 with three proline substitutions in the PKA-binding site does not interact with PKA *in situ*. However, immunoprecipitation with GFP antibody showed the presence of GFP-FL-OPA1 and perilipin in precipitates from cells expressing either GFP-FL-OPA1$^{\#}$ or GFP-FL-OPA1$^{\#}$ AKBmut, indicating that both the wild-type and substituted protein localize normally and interact with perilipin as also shown in the colocalization studies (Figure 5G–I; Supplementary Figures S1C and S2D–F′). Interestingly, the basal phosphorylation state of perilipin as observed with an anti-RXXpS/T antibody was found to be reduced by >90% in immunoprecipitates from cells reconstituted with GFP-FL-OPA1$^{\#}$ AKBmut as compared with cells expressing GFP-FL-OPA1$^{\#}$ (Figure 6D, right panel; $P<0.0025$). This suggests that the absence of PKA anchored to OPA1 affects basal levels of perilipin phosphorylation. Finally, immunoprecipitation of HSL revealed the presence of the same levels of phospho-HSL in precipitates from both GFP-FL-OPA1$^{\#}$ and GFP-FL-OPA1$^{\#}$ AKBmut-transfected cells, indicating that the ability of OPA1 to bind PKA does not influence the basal phosphorylation state of HSL.

Isoproterenol-induced lipolysis in cells reconstituted with OPA1 was next assessed as glycerol release in the media from 3T3-L1 adipocytes transfected with OPA1 siRNA and either GFP-FL-OPA1$^{\#}$ or GFP-FL-OPA1$^{\#}$ AKBmut (Figure 6E). In the presence of 10 nM isoproterenol, a robust glycerol release was observed in cells that had received scrambled siRNA (solid bar), whereas significantly less glycerol was released in cultures treated with OPA1 siRNA (open bar, 51% reduction, $P<0.001$) as also seen in Figure 6B. Moreover, when GFP-FL-OPA1$^{\#}$ was expressed in cells with knockdown of endogenous OPA1, the isoproterenol-induced glycerol release was increased two-fold compared with OPA1 knockdown cells and adrenergic regulation was partially restored ($P<0.001$). In contrast, expression of GFP-FL-OPA1$^{\#}$ AKBmut in OPA1 knockdown cells did not restore isoproterenol-induced glycerol release (57.8% reduction compared with cells transfected with scrambled siRNA, $P<0.001$) and was not significantly different from the level of glycerol release in OPA1 knockdown cells. The fact that GFP-FL-OPA1 expression did not completely rescue the effect of OPA1 knockdown on isoproterenol-induced lipolysis may be due to transfection efficiency of the mammalian expression vector, which was lower than that of the siRNA as observed by GFP fluorescence compared with fluorescence of FITC-labelled siRNA in separate experiments (data not shown).

To examine the role of OPA1 in the control of lipolysis independently of its mitochondrial localization, we next engineered chimeric constructs consisting of the lipid droplet targeting sequence from perilipin (LDTS; amino acids 233–366, notably without any of the four PKA phosphorylation sites as Ser 276 inside the sequence was changed to Ala) (Subramanian *et al*, 2004) fused to OPA1 deleted of the MTS (ΔMTS-OPA1$^{\#}$) that directs the localization of wild-type OPA1 to both mitochondria and lipid droplets (Supplementary Figure S2G–V′) with or without the AKB mutated (perilipin-LDTS ΔMTS-OPA1$^{\#}$ or perilipin-LDTS ΔMTS-OPA1$^{\#}$ AKBmut) and fused to green fluorescent protein in the N- or C-terminal position (see Figure 6E, top for design of fusion proteins). Expression of the chimeric proteins in the absence of endogenous OPA1 revealed colocalization with lipid droplets as evident from correlation analysis of GFP fluorescence with perilipin immunolabelling (correlation coefficients of $R=0.63$–0.66, see Supplementary Figure S3D–F′ for analysis of perilipin-LDTS ΔMTS-OPA1$^{\#}$ AKBmut-GFP and perilipin). In the absence of endogenous OPA1 expression, the two chimeric LDTS-ΔMTS-OPA1 proteins with a functional AKB domain were able to restore isoproterenol-induced glycerol release (both $P<0.001$) compared with OPA1 knockdown cells whereas expression of chimeric constructs with a mutant AKB domain did not (Figure 6E). These data strongly suggest that LD-targeted OPA1 with a functional AKB domain is able to confer adrenergic regulation of perilipin phosphorylation by localizing of PKA independently of the mitochondrial pool of OPA1.

To control for the possibility that changes in glycerol release observed upon manipulations of OPA1 levels were not due merely to changes in the stored amount of TAG available for lipolysis or an effect on lipid droplet integrity,

lipid droplets of OPA1 knockdown cells were examined by immunostaining with perilipin antibody (Figure 6F and H, green) in combination with Oil Red O staining for TAG (Figure 6G and H, red). Lipid droplets in OPA1 knockdown cells were intact and with normal TAG stores. Furthermore, the level of TAG stored in adipocytes after siRNA-mediated OPA1 knockdown and reconstitution with exogenous OPA1 were quantified by staining cell cultures with Oil Red O, washing, extracting the remaining Oil Red O in isopropanol and measuring optical density (Figure 6I). No significant difference in TAG content was observed in adipocytes after siRNA knockdown or OPA1 expression compared with cells transfected with scrambled siRNA. To ensure that siRNA-mediated knockdown and reconstitution experiment did not affect the β-adrenergic signalling pathway or integrity and function of mitochondria, we measured the intracellular cAMP production and the ATP concentration in adipocytes before and after isoproterenol stimulation. Whereas a clear increase of cAMP was observed after stimulation with 10 nM isoproterenol compared with basal levels, no significant difference in intracellular cAMP production was observed after the different transfections (Figure 6J). Moreover, no differences in ATP concentration were observed in cells after siRNA-mediated knockdown and reconstitution experiments (Figure 6K).

Together, our knockdown and reconstitution experiments suggest that OPA1 plays a key role in the regulation of lipolysis by coordinating a signal complex on lipid droplets containing both PKA and perilipin where discretely controlled phosphorylation of perilipin regulates access of lipases to the lipid stores upon adrenergic stimuli.

The dual-specificity AKAP OPA1 permits both type I and type II PKA to regulate lipolysis

A typical feature of AKAP-coordinated phosphorylation events regulating physiological processes is that displacement of the anchored pool of PKA by anchoring disruptor peptides should block regulation by cAMP. The prototypic anchoring disruptor peptide Ht31 derived from AKAP-Lbc (Carr *et al*, 1992) has been extensively used for this type of experiment by offering soluble binding sites for PKA and was already in Figure 1A shown to disrupt isoproterenol-induced perilipin phosphorylation. Ht31 disrupts anchoring of type II PKA, but at somewhat higher concentrations also competes anchoring of type I PKA (Herberg *et al*, 2000; Gold *et al*, 2006; Ruppelt *et al*, 2007). More recently, the development of the high-affinity, isoform-specific anchoring disruptors RI anchoring disruptor (RIAD) and SuperAKAP-*IS* has provided tools to specifically delineate effects mediated by type I or type II PKA (Carlson *et al*, 2006; Gold *et al*, 2006). Here, we used the tool box of anchoring disruptor peptides to further characterize the AKAP coordinating adrenergic control of lipolysis. First, conditions for peptide loading of differentiated adipocytes were established by incubating 3T3-L1 adipocytes with FITC-labelled, poly-arginine-tagged RIAD and SuperAKAP-*IS* peptides at different concentrations and for different time periods. Maximal peptide loading was observed at 120 min (Figure 7A and B, respectively). Furthermore, an optimal peptide concentration of 30 μM was determined by toxicity testing (data not shown). The effect of anchoring disruptors on lipolysis was next analysed by glycerol-release assay. Adipocytes preincubated with Ht31 peptide presented significantly decreased glycerol release after stimulation with 30 or 100 nM isoproterenol compared with mock loaded cells (42% reduction, $P<0.005$; 92% reduction, $P<0.001$, respectively) (Figure 7C). In contrast, 3T3-L1 adipocytes incubated separately with either RIAD (Figure 7D) or SuperAKAP-*IS* peptide (Figure 7E) did not show any significant differences in lipolysis compared with the effect of the corresponding scrambled peptides. However, incubation with a combination of RIAD and SuperAKAP-*IS* peptides (Figure 7F; 30 μM each) effectively blocked isoproterenol-induced glycerol release (74 and 97% decrease at 30 and 100 nM isoproterenol compared with scrambled control with both peptides, $P<0.001$). Our results are compatible with the notion derived from the kinetic data on the PKA–OPA1 association in Figure 2 that OPA1 is a true dual-specificity AKAP that permits both type I and type II PKA to bind and regulate lipolysis (see Figure 7G for depiction of effect of various anchoring disruptors). From this notion it can be derived that if both type I and type II PKA are available for binding to OPA1 (although RI appears to be the preferred binding partner in 3T3-L1 cells), only the combination of RIAD and SuperAKAP-*IS* would compete binding of both forms of PKA and block adrenergic regulation of lipolysis. This is consistent with our observations of hormonally regulated lipolysis in the presence of various anchoring disruptors (Figure 7F and G, bottom right panel).

Discussion

Here, we report the identification of OPA1 as an AKAP for perilipin. OPA1, normally found in mitochondria in other cell types, is expressed at increasing levels during adipocyte differentiation and targeted to lipid droplets where it organizes a supramolecular complex with both PKA and perilipin. We show that OPA1 is necessary for discrete control of perilipin phosphorylation and lipolysis.

The observation that adipocytes expressing the Ht31 anchoring disruptor lacked perilipin phosphorylation upon adrenergic stimulation indicated that AKAP-mediated targeting of PKA was necessary for perilipin phosphorylation. This prompted us to search for an AKAP for perilipin. Several AKAPs have already been identified in adipocytes (Chaudhry *et al*, 2002; Nomura *et al*, 2002; Tao *et al*, 2003; Zhang *et al*,

Figure 7 The dual-specificity function of OPA1 allows redundance in the anchored PKA isozyme regulating lipolysis. (**A**, **B**) Time-dependent (30, 60 or 120 min) peptide loading of 3T3-L1 adipocytes with RIAD-FITC (**A**, green; upper row) or SuperAKAP-*IS*-FITC (**B**, green; upper row) at 15 μM each. Subsequently, 3T3-L1 adipocytes were immunostained for perilipin (red; **A**, **B**, lower rows). Scale bar: 20 μm. (**C**–**F**) Effect of anchoring disruptor peptides in isoproterenol-regulated lipolysis were studied by measuring the amount of glycerol released into media of 3T3-L1 adipocytes after incubation with Ht31 (**C**), RIAD (**D**), SuperAKAP-*IS* (**E**) or RIAD and SuperAKAP-*IS* peptides together (**F**). Stimulation was accomplished by incubation with 30 or 100 nM isoproterenol for 2 h at 72 h of culture. Results are expressed as the mean ± s.e.m. of $n=6$ independent experiments (***$P<0.001$ and **$P<0.01$). (**G**) Schematic illustration of the effect of specific anchoring disruptor peptides on lipolysis. (Left) Model of OPA1 as an AKAP organizing activation of lipolysis upon adrenergic stimulation. (Middle row) Model for effect of RIAD or SuperAKAP-*IS* on lipolysis. (Right row) Effect of Ht31 or RIAD and SuperAKAP-*IS* together on adrenergic regulation of lipolysis.

2005; Bridges *et al*, 2006). According to Tao *et al* (2003), a complex formed of the β-AR, an AKAP and PKA is involved in receptor internalization, resensitization and recycling of the β-AR in adipocytes. Although some observations suggested that the association between β-AR and PKA in adipocytes is mediated by AKAP150 or gravin (Fraser *et al*, 2000; Tao *et al*,

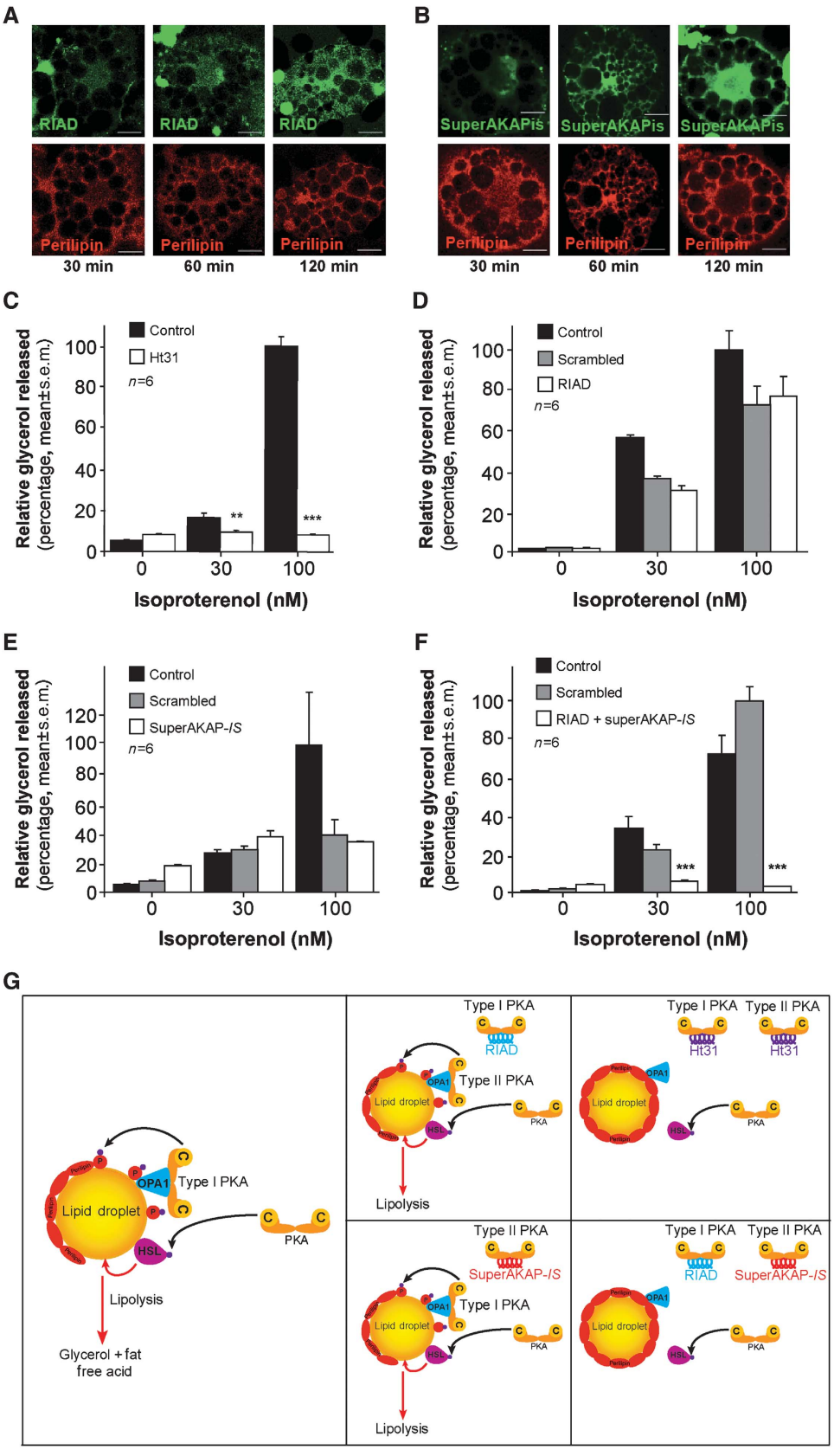

2003), Zhang *et al* (2005) proposed the involvement of a yet unidentified AKAP. Moreover, the compartmentalization of HSL with AKAP150 and PKA has been described to be required for the induction of lipolysis by controlling HSL phosphorylation (Nomura *et al*, 2002), but the importance of this observation is challenged by the more recent reports that HSL is dispensable in catecholamine-stimulated lipolysis. A more recent work proposed D-AKAP1 as a major adipocyte PKA-binding protein and discussed the possibility of D-AKAP1 as a lipid droplet AKAP, but failed to convincingly demonstrate an association with lipid droplets and did not show data to support any functional effect of D-AKAP1 (Bridges *et al*, 2006). Furthermore, Chaudhry *et al* (2002) showed that D-AKAP1 is associated with mitochondria in differentiated adipocytes. In summary, no AKAP has previously been clearly shown to be associated with lipid droplets and to be involved in the regulation of the lipolytic process.

We report here for the first time that OPA1 is a dual-specificity AKAP targeted to lipid droplets in adipocytes. An amphipathic helix AKB domain localized in the C-terminal part of OPA1 is able to bind both type I and type II PKA with low nanomolar affinities. While most dual-specificity AKAPs appear to have lower affinity for type I than for type II PKA due to a faster off-rate of RI (Herberg *et al*, 2000), OPA1 appears to display equal affinities for both isozymes or even a slightly higher affinity for type I PKA. Our kinetic analysis demonstrated that this was due to similar on- and off-rates of both isozymes. When the affinity of an AKAP for type I and type II PKA is similar, the availability of the two isozymes would be expected to determine association. Indeed, in 3T3-L1 cells that express both RIα and RIIβ, we observed that PKA type I associated with OPA1 and controlled lipolysis. In contrast, OPA1 was associated with RIIβ in WAT, where it is the predominantly expressed R subunit and where type II PKA has been reported to control lipolysis (Beebe *et al*, 1984; Robinson-Steiner *et al*, 1984). Whether lipolysis is controlled by type I or type II PKA is clearly important as K_{act} for the two isozymes differ (50–100 and 200–400 nM for type I and type II, respectively). This, in turn, affects the sensitivity to catecholamine-stimulated lipolysis as illustrated in the RIIβ null-mutant mice where rescue by upregulation of RIα provides a type I PKA to control lipolysis and results in lean mice (Cummings *et al*, 1996). Furthermore, regulation of RIα levels may be a means to control adipocyte sensitivity to cAMP-regulated lipolysis. This is illustrated in mice with high levels of expression of FoxC2 that controls RIα expression resulting in mice protected against diet-induced obesity and insulin resistance (Cederberg *et al*, 2001).

OPA1 is earlier reported to be expressed in different cell types with phenotypes of mutations in the *opa1* gene related to its function in the nervous system. Here, we show that OPA1 is expressed in WAT and BAT and upregulated during adipocyte differentiation at a time consistent with its regulation by adipocyte-specific transcription factors such as PPARγ. The dynamin-related GTPase OPA1 is reported to be targeted to the mitochondrial membrane in different cell types including adipocytes (Misaka *et al*, 2002; Olichon *et al*, 2002; Satoh *et al*, 2003; Kita *et al*, 2009) and involved in mitochondrial fusion and apoptosis through mitochondrial cristae remodelling (Olichon *et al*, 2003; Cipolat *et al*, 2004; Frezza *et al*, 2006; Ishihara *et al*, 2006). By transfection of COS-7 cells with the 30, 60 or 90 N-terminal amino acids of the OPA1 MTS fused to the N-terminal end of EGFP, amino acids 30–90 of the MTS were shown to be important for the mitochondrial location (Misaka *et al*, 2002; Olichon *et al*, 2002; Satoh *et al*, 2003; Kita *et al*, 2009). In contrast, our immunolocalization and cell fractionation studies in adipocytes revealed that a substantial fraction of OPA1 is associated with lipid droplets and that amino acids 1–30 of the OPA1 MTS appeared to be required for OPA1 to access lipid droplets. Furthermore, deletion of amino acids 30–87 also reduced lipid droplet targeting of OPA1, although not to the same extent as its mitochondrial targeting. The differences in subcellular distribution may reflect that the lipophilic nature of the OPA1 membrane targeting domain favour its association with lipid droplets in cell types where these are available. Transport of OPA1 to lipid droplets may occur via a direct route to lipid droplets in parallel with the mitochondrial targeting (dual targeting) or by an indirect route via mitochondria. While the observation that deletion of the full 90 amino acids of the OPA1 MTS lead to loss of both and lipid droplet targeting may point towards the mitochondrial transit route, the fact that lipid droplet targeting was lost also upon deletion of the first 30 amino acids of the MTS that have been shown to be less important for mitochondrial targeting may indicate distinct targeting mechanisms. However, the targeting mechanism could not be readily defined and requires future investigation in more detail.

Two recent papers indicate that OPA1 may be redistributed from mitochondria to membrane tubulations extending from mitochondria (Ban *et al*, 2010) or lost during ER stress (Zhang *et al*, 2008), indicating some mobility of OPA1. It is interesting to speculate that OPA1 localized on both mitochondria and lipid droplets could coordinate the positioning of lipid droplets in close proximity to mitochondria to facilitate the supply of FFA from lipolysis to mitochondria for ATP synthesis. Silencing of mitochondrial fusion proteins such as mitofusin 2 in adipocytes lead to accumulation of lipid droplets, whereas silencing of fission proteins such as Drp1 is responsible of a decrease in TAG content (Kita *et al*, 2009), indicating interplay between mitochondrial dynamics and lipid storage in adipocytes. Our findings indicate that the silencing of OPA1 has a distinct effect as it does not impact lipid droplet accumulation or lipid content of adipocytes, but affects the adrenergic regulation of the lipolysis.

In addition to binding PKA, our data also showed that OPA1 bound perilipin, consistent with observations made with other macromolecular complexes organized by AKAPs that include the substrate for PKA as well as other signalling enzymes (Tasken and Aandahl, 2004; Wong and Scott, 2004). While preliminary data indicate a direct interaction between OPA1 and perilipin, the molecular determinants for interaction and possible presence of other signalling enzymes in the OPA1-scaffolded macromolecular complex remain to be investigated. Furthermore, the function of OPA1 in adipocyte mitochondria and the possibility of OPA1 functioning as an AKAP also in mitochondria in different cell types would be interesting to pursue in future studies.

By silencing and reconstitution experiments, we demonstrated a central role for OPA1 in catecholamine-stimulated lipolysis. siRNA-mediated knockdown of OPA1 induced a decrease in isoproterenol-induced lipolysis, while reconstitution experiments with siRNA-resistant wild-type OPA1

rescued this effect. Moreover, reconstitution experiments using a mutated construct substituted in the AKB domain, so that it cannot associate with PKA, did not rescue isoproterenol-induced lipolysis. Finally, reconstitution experiments with OPA1 deleted of its mitochondrial and lipid droplet targeting sequences but fused to a lipid droplet targeting domain also reconstituted adrenergic regulation of lipolysis when the AKB domain was present. Recent work revealed that loss of function of OPA1 increased mitochondrial fragmentation without altering bioenergetics or increasing apoptosis (Spinazzi *et al*, 2008), which would indicate that the loss of isoproterenol-stimulated lipolysis observed after OPA1 silencing in adipocytes is not due to induction of apoptosis. Nor was this lack in response to adrenergic stimulation due to a deficiency in substrate for lipolysis, as we observed no decrease in lipid droplet TAG content. Together with the reconstitution experiments, this indicates that it is the loss of PKA from the perilipin/OPA1 macromolecular complex, which prevents perilipin phosphorylation. The silencing of OPA1 and reconstitution experiments had no effect on HSL phosphorylation, supporting the hypothesis of another AKAP controlling the HSL phosphorylation state (Nomura *et al*, 2002). The silencing of OPA1 also led to a decrease in perilipin protein levels consistent with the notion that absence of one of the partners of the complex could destabilize the remainder. Indeed, it has been confirmed recently in other models that the knockdown of a protein may affect the stability of other protein partners present in the same supramolecular complex (Oswald *et al*, 2009). Here, however, perilipin levels appeared to be rescued by an upregulation of ADRP (Supplementary Figure S4), in line with earlier studies (Tansey *et al*, 2001).

We employed a strategy of PKA displacement using anchoring disruptor peptides to confirm the presence and role of a dual-specificity AKAP in regulation of lipolysis. Our results obtained with Ht31 are in agreement with a previous study showing decreased catecholamine-stimulated lipolysis in cells loaded with Ht31 (Nomura *et al*, 2002; Zhang *et al*, 2005). Furthermore, we show that RIAD and SuperAKAP-*IS* that selectively displace either type I or type II PKA did not inhibit isoproterenol-stimulated lipolysis when added separately, whereas the combination reduced regulation of lipolysis to the same extent as Ht31. These results allow us to propose a model to explain the adrenergic control of lipolysis (Figure 7G). In 3T3-L1 adipocytes, OPA1 is located in a supramolecular complex associated with lipid droplets, which keeps type I PKA preferentially in close proximity to perilipin to control its phosphorylation state during adrenergic stimulation. Phosphorylation of perilipin through the OPA1/PKA complex stimulates lipolysis by allowing access of lipases to TAG in lipid droplets. Interestingly, it is necessary to block the dual-specificity function of OPA1 to abolish stimulation of lipolysis as there is redundancy with respect to the use of different PKA isoforms, although the use of PKA type I versus PKA type II affects the sensitivity of the process to catecholamines.

In addition to control the supply of energy in the fed versus the fasting state, control of lipolysis is important to provide FFA for hepatic synthesis of TAG-containing lipoproteins. Furthermore, alterations in lipolysis are frequently observed in obesity, which is increasing rapidly in the industrialized part of the world and constitutes a growing medical problem. Obesity, characterized primarily by an excess of WAT, results in metabolic syndrome, which encompasses insulin resistance and hypertension and leads to type II diabetes, atherosclerosis and cardiovascular disease (Kahn *et al*, 2000; Unger, 2003). At the cellular level, obesity leads to a pathological accumulation of TAG and an enlargement of adipocyte size, as well as increased numbers of adipocytes. Consequently, understanding the regulation of lipolysis and its dysregulation are highly interesting in the context of obesity.

In summary, we report a new function for the OPA1 protein as a dual-specificity AKAP associated with lipid droplets in adipocytes whose role is to coordinate a supramolecular signal complex at the surface of lipid droplets. We provide direct evidence that OPA1 mediates the adrenergic control of lipolysis by providing PKA in close proximity of perilipin to regulate its phosphorylation state and thereby control lipolysis.

Materials and methods

Cell culture

3T3-L1 cells (ATCC) were cultured as described previously (Enrique-Tarancon *et al*, 1998) (see Supplementary data).

Protein sample preparation and immunoblot analysis

Total cell lysates were prepared in lysis buffer (see Supplementary data) and proteins were resolved by SDS–PAGE and blotted onto nitrocellulose membranes. The resulting filters were immunoblotted with antibodies to OPA1 (0.25 μg/ml; BD Biosciences), perilipin (1:1000; Fitzerald Industries from both rabbit and guinea pig), HSL (1:1000; Cell Signaling), phospho-HSL (1:1000; Cell Signaling), PKA-RIα (0.25 μg/ml; BD Biosciences), PKA-RIIβ (0.25 μg/ml; BD Biosciences), phospho-PKA substrate (anti-RRXpS/T, 1:2000, Cell Signaling), mitofilin (1:2000; AbCam), mitofusin2 (1 μg/ml; AbCam), pyruvate dehydrogenase E1β subunit (1 μg/ml; AbCam) ADRP and TIP47 (1/1000 each; gift from Dr KT Dalen). After incubation with appropriate HRP-conjugated secondary antibody, blots were developed by using Supersignal West Pico substrate (Pierce).

Immunoprecipitation

Protein A/G plus agarose (Santa Cruz Biotechnology) was absorbed with antibody against OPA1 (BD Biosciences), perilipin (Fitzgerald Industries) or PKA-RIα or -RIIβ (both BD Biosciences) or left without antibody. Total cell lysates were prepared as above, added to the protein A/G agarose immunocomplex and incubated overnight at 4 °C on a rocker platform. Immunocomplexes were washed five times in lysis buffer before SDS–PAGE and immunoblotting with the indicated antibodies.

Lipid droplet purification

Lipid droplets were purified as described previously (Brasaemle *et al*, 2004) (see Supplementary data).

R-overlays

R-overlays were performed as described previously (Hausken *et al*, 1998) by using ^{32}P-labelled recombinant RII or RI (A98S) substituted to allow autophosphorylation (Durgerian and Taylor, 1989) (see Supplementary data).

Immunolocalization studies

Immunofluorescence staining was performed on differentiated 3T3-L1. Cells were fixed for 15 min in 3% paraformaldehyde, permeabilized for 15 min with 0.1% saponin and blocked for 20 min in 3% fatty acid-free BSA, 0.2 M glycine and 0.1% saponin. Primary antibodies anti-OPA1 (2.5 μg/ml; BD Biosciences), anti-perilipin (1:100; Fitzerald Industries from guinea pig), anti-HSL (1:100; Cell Signaling), anti-PKA-RIα (2.5 μg/ml; BD Biosciences), anti-PKA-RIIβ (2.5 μg/ml; BD Biosciences) and mitofusin2 (20 μg/ml; AbCam) were prepared in PBS with 0.01% Tween 20 (PBS-T), 3% BSA, 0.1% saponin and incubated overnight at 4 °C. Cells were next incubated with the appropriate fluorochrome-conjugated

secondary antibodies (Alexa Fluor 488 and Alexa Fluor 546 (1:1000; Invitrogen)) in PBS-T, 0.1% saponin for 1 h. Controls without primary antibody or with nonspecific IgG of the same isotype were all negative (data not shown). See also Supplementary data.

siRNA, mammalian expression vectors and transfection

siRNA transfection was performed using Lipofectamine 2000 CD reagent (Invitrogen) according to the manufacturer's protocol. See also Supplementary data.

The mammalian transfection vectors were introduced into 3T3-L1 adipocytes by using Fugene 6 transfection reagent (Roche) according to the manufacturer's protocol. See also Supplementary data.

Lipolysis assay

Differentiated 3T3-L1 cells were incubated in DMEM (without phenol red) containing 2% fatty acid-free BSA overnight. Cells were stimulated in fresh media with or without isoproterenol (5–100 nM) for lipolysis assays. After 2 h of incubation, 50 μl of medium was withdrawn and used for the assay. Glycerol levels were determined using the Free Glycerol Determination Kit (Sigma-Aldrich) according to the manufacturer's instruction.

Statistics

Quantitative data are presented as mean ± s.e.m. Differences were identified by analysis of variance and considered significant when $P<0.05$. See also Supplementary data.

Supplementary data

Supplementary data are available at *The EMBO Journal* Online (http://www.embojournal.org).

Acknowledgements

This work was supported by grants from the Norwegian Functional Genomics Program, The Research Council of Norway, Novo Nordic Foundation and the European Union (Grant no. 037189, thera-cAMP). We are grateful to Jorun Solheim and Gladys M Tjørhom for technical assistance, to Ola Blingsmo for peptide synthesis, to Dr Sven Enerbäck for gift of a plasmid with the AP1 promoter, to Dr John D Scott for gift of expression vectors for Ht31, to Dr Ruth Valgardsdottir for gift of ΔMDDX28 plasmid, to Dr Mohammed Amarzguioui for help with OPA1 siRNA design, to Dr Erwan Delbarre for help with colocalization analysis and Drs Line M Grønning Wang and Knut T Dalen for helpful comments and input on various parts of the work.

Author contributions: GP, OW, EJ, LM and AJS did the experiments and analysed the data; KT supervised the project; HU and TK provided essential technologies and analysed the data; and GP, OW and KT wrote the paper. All authors read and commented on the draft versions of the manuscript and approved the final version.

Conflict of interest

The authors declare that they have no conflict of interest.

References

Alexander C, Votruba M, Pesch UE, Thiselton DL, Mayer S, Moore A, Rodriguez M, Kellner U, Leo-Kottler B, Auburger G, Bhattacharya SS, Wissinger B (2000) OPA1, encoding a dynamin-related GTPase, is mutated in autosomal dominant optic atrophy linked to chromosome 3q28. *Nat Genet* **26:** 211–215

Ban T, Heymann JA, Song Z, Hinshaw JE, Chan DC (2010) OPA1 disease alleles causing dominant optic atrophy have defects in cardiolipin-stimulated GTP hydrolysis and membrane tubulation. *Hum Mol Genet* **19:** 2113–2122

Beebe SJ, Holloway R, Rannels SR, Corbin JD (1984) Two classes of cAMP analogs which are selective for the two different cAMP-binding sites of type II protein kinase demonstrate synergism when added together to intact adipocytes. *J Biol Chem* **259:** 3539–3547

Blanchette-Mackie EJ, Dwyer NK, Barber T, Coxey RA, Takeda T, Rondinone CM, Theodorakis JL, Greenberg AS, Londos C (1995) Perilipin is located on the surface layer of intracellular lipid droplets in adipocytes. *J Lipid Res* **36:** 1211–1226

Bolte S, Cordelieres FP (2006) A guided tour into subcellular colocalization analysis in light microscopy. *J Microsc* **224:** 213–232

Brasaemle DL, Dolios G, Shapiro L, Wang R (2004) Proteomic analysis of proteins associated with lipid droplets of basal and lipolytically stimulated 3T3-L1 adipocytes. *J Biol Chem* **279:** 46835–46842

Brasaemle DL, Levin DM, Adler-Wailes DC, Londos C (2000a) The lipolytic stimulation of 3T3-L1 adipocytes promotes the translocation of hormone-sensitive lipase to the surfaces of lipid storage droplets. *Biochim Biophys Acta* **1483:** 251–262

Brasaemle DL, Rubin B, Harten IA, Gruia-Gray J, Kimmel AR, Londos C (2000b) Perilipin A increases triacylglycerol storage by decreasing the rate of triacylglycerol hydrolysis. *J Biol Chem* **275:** 38486–38493

Bridges D, MacDonald JA, Wadzinski B, Moorhead GB (2006) Identification and characterization of D-AKAP1 as a major adipocyte PKA and PP1 binding protein. *Biochem Biophys Res Commun* **346:** 351–357

Carlson CR, Lygren B, Berge T, Hoshi N, Wong W, Tasken K, Scott JD (2006) Delineation of type I protein kinase A-selective signaling events using an RI anchoring disruptor. *J Biol Chem* **281:** 21535–21545

Carr DW, Hausken ZE, Fraser ID, Stofko-Hahn RE, Scott JD (1992) Association of the type II cAMP-dependent protein kinase with a human thyroid RII-anchoring protein. Cloning and characterization of the RII-binding domain. *J Biol Chem* **267:** 13376–13382

Cederberg A, Gronning LM, Ahren B, Tasken K, Carlsson P, Enerback S (2001) FOXC2 is a winged helix gene that counteracts obesity, hypertriglyceridemia, and diet-induced insulin resistance. *Cell* **106:** 563–573

Chaudhry A, Zhang C, Granneman JG (2002) Characterization of RII(beta) and D-AKAP1 in differentiated adipocytes. *Am J Physiol Cell Physiol* **282:** C205–C212

Cipolat S, Martins de Brito O, Dal Zilio B, Scorrano L (2004) OPA1 requires mitofusin 1 to promote mitochondrial fusion. *Proc Natl Acad Sci USA* **101:** 15927–15932

Cummings DE, Brandon EP, Planas JV, Motamed K, Idzerda RL, McKnight GS (1996) Genetically lean mice result from targeted disruption of the RII beta subunit of protein kinase A. *Nature* **382:** 622–626

Delettre C, Lenaers G, Griffoin JM, Gigarel N, Lorenzo C, Belenguer P, Pelloquin L, Grosgeorge J, Turc-Carel C, Perret E, Astarie-Dequeker C, Lasquellec L, Arnaud B, Ducommun B, Kaplan J, Hamel CP (2000) Nuclear gene OPA1, encoding a mitochondrial dynamin-related protein, is mutated in dominant optic atrophy. *Nat Genet* **26:** 207–210

Diviani D, Scott JD (2001) AKAP signaling complexes at the cytoskeleton. *J Cell Sci* **114:** 1431–1437

Durgerian S, Taylor SS (1989) The consequences of introducing an autophosphorylation site into the type I regulatory subunit of cAMP-dependent protein kinase. *J Biol Chem* **264:** 9807–9813

Enrique-Tarancon G, Marti L, Morin N, Lizcano JM, Unzeta M, Sevilla L, Camps M, Palacin M, Testar X, Carpene C, Zorzano A (1998) Role of semicarbazide-sensitive amine oxidase on glucose transport and GLUT4 recruitment to the cell surface in adipose cells. *J Biol Chem* **273:** 8025–8032

Fain JN, Garcija-Sainz JA (1983) Adrenergic regulation of adipocyte metabolism. *J Lipid Res* **24:** 945–966

Fraser ID, Cong M, Kim J, Rollins EN, Daaka Y, Lefkowitz RJ, Scott JD (2000) Assembly of an A kinase-anchoring protein-beta(2)-adrenergic receptor complex facilitates receptor phosphorylation and signaling. *Curr Biol* **10:** 409–412

Fredrikson G, Tornqvist H, Belfrage P (1986) Hormone-sensitive lipase and monoacylglycerol lipase are both required for complete degradation of adipocyte triacylglycerol. *Biochim Biophys Acta* **876:** 288–293

Frezza C, Cipolat S, Martins de Brito O, Micaroni M, Beznoussenko GV, Rudka T, Bartoli D, Polishuck RS, Danial NN, De Strooper B, Scorrano L (2006) OPA1 controls apoptotic cristae remodeling independently from mitochondrial fusion. *Cell* **126:** 177–189

Giudicelli H, Combes-Pastre N, Boyer J (1974) Lipolytic activity of adipose tissue. IV. The diacylglycerol lipase activity of human adipose tissue. *Biochim Biophys Acta* **369:** 25–33

Gold MG, Lygren B, Dokurno P, Hoshi N, McConnachie G, Tasken K, Carlson CR, Scott JD, Barford D (2006) Molecular basis of AKAP specificity for PKA regulatory subunits. *Mol Cell* **24:** 383–395

Greenberg AS, Egan JJ, Wek SA, Garty NB, Blanchette-Mackie EJ, Londos C (1991) Perilipin, a major hormonally regulated adipocyte-specific phosphoprotein associated with the periphery of lipid storage droplets. *J Biol Chem* **266:** 11341–11346

Greenberg AS, Egan JJ, Wek SA, Moos Jr MC, Londos C, Kimmel AR (1993) Isolation of cDNAs for perilipins A and B: sequence and expression of lipid droplet-associated proteins of adipocytes. *Proc Natl Acad Sci USA* **90:** 12035–12039

Haemmerle G, Zimmermann R, Hayn M, Theussl C, Waeg G, Wagner E, Sattler W, Magin TM, Wagner EF, Zechner R (2002) Hormone-sensitive lipase deficiency in mice causes diglyceride accumulation in adipose tissue, muscle, and testis. *J Biol Chem* **277:** 4806–4815

Hausken ZE, Coghlan VM, Scott JD (1998) Overlay, ligand blotting, and band-shift techniques to study kinase anchoring. *Methods Mol Biol* **88:** 47–64

Herberg FW, Maleszka A, Eide T, Vossebein L, Tasken K (2000) Analysis of A-kinase anchoring protein (AKAP) interaction with protein kinase A (PKA) regulatory subunits: PKA isoform specificity in AKAP binding. *J Mol Biol* **298:** 329–339

Ishihara N, Fujita Y, Oka T, Mihara K (2006) Regulation of mitochondrial morphology through proteolytic cleavage of OPA1. *EMBO J* **25:** 2966–2977

Jarnaess E, Ruppelt A, Stokka AJ, Lygren B, Scott JD, Tasken K (2008) Dual specificity A-kinase anchoring proteins (AKAPs) contain an additional binding region that enhances targeting of protein kinase A type I. *J Biol Chem* **283:** 33708–33718

Jenkins CM, Mancuso DJ, Yan W, Sims HF, Gibson B, Gross RW (2004) Identification, cloning, expression, and purification of three novel human calcium-independent phospholipase A2 family members possessing triacylglycerol lipase and acylglycerol transacylase activities. *J Biol Chem* **279:** 48968–48975

Kahn CR, Chen L, Cohen SE (2000) Unraveling the mechanism of action of thiazolidinediones. *J Clin Invest* **106:** 1305–1307

Kimmel AR, Brasaemle DL, McAndrews-Hill M, Sztalryd C, Londos C (2009) Adoption of PERILIPIN as a unifying nomenclature for the mammalian PAT-family of intracellular, lipid storage droplet proteins. *J Lipid Res* **51:** 468–471

Kinderman FS, Kim C, von Daake S, Ma Y, Pham BQ, Spraggon G, Xuong NH, Jennings PA, Taylor SS (2006) A dynamic mechanism for AKAP binding to RII isoforms of cAMP-dependent protein kinase. *Mol Cell* **24:** 397–408

Kita T, Nishida H, Shibata H, Niimi S, Higuti T, Arakaki N (2009) Possible role of mitochondrial remodelling on cellular triacylglycerol accumulation. *J Biochem* **146:** 787–796

Londos C, Brasaemle DL, Schultz CJ, Segrest JP, Kimmel AR (1999) Perilipins, ADRP, and other proteins that associate with intracellular neutral lipid droplets in animal cells. *Semin Cell Dev Biol* **10:** 51–58

Michel JJ, Scott JD (2002) AKAP mediated signal transduction. *Annu Rev Pharmacol Toxicol* **42:** 235–257

Misaka T, Miyashita T, Kubo Y (2002) Primary structure of a dynamin-related mouse mitochondrial GTPase and its distribution in brain, subcellular localization, and effect on mitochondrial morphology. *J Biol Chem* **277:** 15834–15842

Nomura S, Kawanami H, Ueda H, Kizaki T, Ohno H, Izawa T (2002) Possible mechanisms by which adipocyte lipolysis is enhanced in exercise-trained rats. *Biochem Biophys Res Commun* **295:** 236–242

Olichon A, Baricault L, Gas N, Guillou E, Valette A, Belenguer P, Lenaers G (2003) Loss of OPA1 perturbates the mitochondrial inner membrane structure and integrity, leading to cytochrome c release and apoptosis. *J Biol Chem* **278:** 7743–7746

Olichon A, Emorine LJ, Descoins E, Pelloquin L, Brichese L, Gas N, Guillou E, Delettre C, Valette A, Hamel CP, Ducommun B, Lenaers G, Belenguer P (2002) The human dynamin-related protein OPA1 is anchored to the mitochondrial inner membrane facing the inter-membrane space. *FEBS Lett* **523:** 171–176

Osuga J, Ishibashi S, Oka T, Yagyu H, Tozawa R, Fujimoto A, Shionoiri F, Yahagi N, Kraemer FB, Tsutsumi O, Yamada N (2000) Targeted disruption of hormone-sensitive lipase results in male sterility and adipocyte hypertrophy, but not in obesity. *Proc Natl Acad Sci USA* **97:** 787–792

Oswald C, Krause-Buchholz U, Rodel G (2009) Knockdown of human COX17 affects assembly and supramolecular organization of cytochrome c oxidase. *J Mol Biol* **389:** 470–479

Pidoux G, Tasken K (2010) Specificity and spatial dynamics of PKA signaling organized by A kinase anchoring proteins. *J Mol Endocrinol* **44:** 271–284

Robinson-Steiner AM, Beebe SJ, Rannels SR, Corbin JD (1984) Microheterogeneity of type II cAMP-dependent protein kinase in various mammalian species and tissues. *J Biol Chem* **259:** 10596–10605

Ruppelt A, Mosenden R, Gronholm M, Aandahl EM, Tobin D, Carlson CR, Abrahamsen H, Herberg FW, Carpen O, Tasken K (2007) Inhibition of T cell activation by cyclic adenosine 5′-monophosphate requires lipid raft targeting of protein kinase A type I by the A-kinase anchoring protein ezrin. *J Immunol* **179:** 5159–5168

Satoh M, Hamamoto T, Seo N, Kagawa Y, Endo H (2003) Differential sublocalization of the dynamin-related protein OPA1 isoforms in mitochondria. *Biochem Biophys Res Commun* **300:** 482–493

Sesaki H, Southard SM, Yaffe MP, Jensen RE (2003) Mgm1p, a dynamin-related GTPase, is essential for fusion of the mitochondrial outer membrane. *Mol Biol Cell* **14:** 2342–2356

Soni KG, Lehner R, Metalnikov P, O'Donnell P, Semache M, Gao W, Ashman K, Pshezhetsky AV, Mitchell GA (2004) Carboxylesterase 3 (EC 3.1.1.1) is a major adipocyte lipase. *J Biol Chem* **279:** 40683–40689

Souza SC, Muliro KV, Liscum L, Lien P, Yamamoto MT, Schaffer JE, Dallal GE, Wang X, Kraemer FB, Obin M, Greenberg AS (2002) Modulation of hormone-sensitive lipase and protein kinase A-mediated lipolysis by perilipin A in an adenoviral reconstituted system. *J Biol Chem* **277:** 8267–8272

Spinazzi M, Cazzola S, Bortolozzi M, Baracca A, Loro E, Casarin A, Solaini G, Sgarbi G, Casalena G, Cenacchi G, Malena A, Frezza C, Carrara F, Angelini C, Scorrano L, Salviati L, Vergani L (2008) A novel deletion in the GTPase domain of OPA1 causes defects in mitochondrial morphology and distribution, but not in function. *Hum Mol Genet* **17:** 3291–3302

Stokka AJ, Gesellchen F, Carlson CR, Scott JD, Herberg FW, Tasken K (2006) Characterization of A-kinase-anchoring disruptors using a solution-based assay. *Biochem J* **400:** 493–499

Subramanian V, Garcia A, Sekowski A, Brasaemle DL (2004) Hydrophobic sequences target and anchor perilipin A to lipid droplets. *J Lipid Res* **45:** 1983–1991

Tansey JT, Huml AM, Vogt R, Davis KE, Jones JM, Fraser KA, Brasaemle DL, Kimmel AR, Londos C (2003) Functional studies on native and mutated forms of perilipins. A role in protein kinase A-mediated lipolysis of triacylglycerols. *J Biol Chem* **278:** 8401–8406

Tansey JT, Sztalryd C, Gruia-Gray J, Roush DL, Zee JV, Gavrilova O, Reitman ML, Deng CX, Li C, Kimmel AR, Londos C (2001) Perilipin ablation results in a lean mouse with aberrant adipocyte lipolysis, enhanced leptin production, and resistance to diet-induced obesity. *Proc Natl Acad Sci USA* **98:** 6494–6499

Tao J, Wang HY, Malbon CC (2003) Protein kinase A regulates AKAP250 (gravin) scaffold binding to the beta2-adrenergic receptor. *EMBO J* **22:** 6419–6429

Tasken K, Aandahl EM (2004) Localized effects of cAMP mediated by distinct routes of protein kinase A. *Physiol Rev* **84:** 137–167

Tornqvist H, Belfrage P (1976) Purification and some properties of a monoacylglycerol-hydrolyzing enzyme of rat adipose tissue. *J Biol Chem* **251:** 813–819

Unger RH (2003) Minireview: weapons of lean body mass destruction: the role of ectopic lipids in the metabolic syndrome. *Endocrinology* **144:** 5159–5165

Villena JA, Roy S, Sarkadi-Nagy E, Kim KH, Sul HS (2004) Desnutrin, an adipocyte gene encoding a novel patatin domain-containing protein, is induced by fasting and glucocorticoids: ectopic expression of desnutrin increases triglyceride hydrolysis. *J Biol Chem* **279:** 47066–47075

Wang SP, Laurin N, Himms-Hagen J, Rudnicki MA, Levy E, Robert MF, Pan L, Oligny L, Mitchell GA (2001) The adipose tissue phenotype of hormone-sensitive lipase deficiency in mice. *Obes Res* **9:** 119–128

Wong W, Scott JD (2004) AKAP signalling complexes: focal points in space and time. *Nat Rev Mol Cell Biol* **5:** 959–970

Zhang D, Lu C, Whiteman M, Chance B, Armstrong JS (2008) The mitochondrial permeability transition regulates cytochrome c release for apoptosis during endoplasmic reticulum stress by remodeling the cristae junction. *J Biol Chem* **283:** 3476–3486

Zhang J, Hupfeld CJ, Taylor SS, Olefsky JM, Tsien RY (2005) Insulin disrupts beta-adrenergic signalling to protein kinase A in adipocytes. *Nature* **437:** 569–573

Zimmermann R, Haemmerle G, Wagner EM, Strauss JG, Kratky D, Zechner R (2003) Decreased fatty acid esterification compensates for the reduced lipolytic activity in hormone-sensitive lipase-deficient white adipose tissue. *J Lipid Res* **44:** 2089–2099

Zimmermann R, Strauss JG, Haemmerle G, Schoiswohl G, Birner-Gruenberger R, Riederer M, Lass A, Neuberger G, Eisenhaber F, Hermetter A, Zechner R (2004) Fat mobilization in adipose tissue is promoted by adipose triglyceride lipase. *Science* **306:** 1383–1386